

# Implementation of Nickel and Copper as Cost-Effective Alternative Contacts in Silicon Solar Cells

Veysel Unsur<sup>1</sup>

<sup>1</sup>Necmettin Erbakan University

June 11, 2023

## Abstract

Efficient metal contact formation is pivotal for the production of cost-effective, high-performance crystalline silicon (Si) solar cells. Traditionally, screen-printed silver (Ag) contacts on the front surface have dominated the industry, owing to their simplicity, high throughput, and significant electrical benefits. However, the high cost associated with using over 13-20mg/Wp of Ag can impede the development of truly cost-effective solar cells. Therefore, there is an urgent need to explore alternative, economically viable metals compatible with silicon substrates. This study reports on the application of a contact stack consisting of Ag, nickel (Ni), and copper (Cu) in Si solar cells. To prevent Schottky contact formation, Ag is implemented as a seed layer, while Ni and Cu form the metal bulk layer. The fabricated bi-layer stack without selective emitter exhibits a maximum efficiency of ~21.5%, a fill factor of 81.5%, and an average contact resistance of 5.88mΩ·cm<sup>2</sup> for a monofacial PERC cell. Microstructure analysis demonstrate that the metals within the contacts remain distinct, and Cu diffusion into the silicon during the firing process is absent. Consequently, printed bi-layer contacts emerge as a promising alternative to Ag contacts, reducing the Ag consumption to below 2.5mg/Wp per cell without compromising overall efficiency.

Veysel Unsur<sup>1, 2, \*</sup>

<sup>1</sup> Department of Fundamental Sciences, Necmettin Erbakan University, Konya, Türkiye

<sup>2</sup> Center of Solar Energy Research and Applications, ODTÜ-GÜNAM, Ankara, Türkiye

\*Corresponding author: [vunsur@erbakan.edu.tr](mailto:vunsur@erbakan.edu.tr) , [veysel.unsur@odtugunam.org](mailto:veysel.unsur@odtugunam.org)

## Abstract

Efficient metal contact formation is pivotal for the production of cost-effective, high-performance crystalline silicon (Si) solar cells. Traditionally, screen-printed silver (Ag) contacts on the front surface have dominated the industry, owing to their simplicity, high throughput, and significant electrical benefits. However, the high cost associated with using over 13-20mg/Wp of Ag can impede the development of truly cost-effective solar cells. Therefore, there is an urgent need to explore alternative, economically viable metals compatible with silicon substrates. This study reports on the application of a contact stack consisting of Ag, nickel (Ni), and copper (Cu) in Si solar cells. To prevent Schottky contact formation, Ag is implemented as a seed layer, while Ni and Cu form the metal bulk layer. The fabricated bi-layer stack without selective emitter exhibits a maximum efficiency of ~21.5%, a fill factor of 81.5%, and an average contact resistance of 5.88mΩ·cm<sup>2</sup> for a monofacial PERC cell. Microstructure analysis demonstrate that the metals within the contacts remain distinct, and Cu diffusion into the silicon during the firing process is absent. Consequently, printed bi-layer contacts emerge as a promising alternative to Ag contacts, reducing the Ag consumption to below 2.5mg/Wp per cell without compromising overall efficiency.

**Keywords:** PERC, screen printing, alternative metallization, Ni contacts, Cu contacts, solar cells

## Introduction

Screen-printed silver (Ag) metal contacts have long been favored in the production of silicon (Si) solar cells due to their simplicity, maturity, and high throughput. Their dominance in the photovoltaic (PV) market is largely due to their excellent conductivity and solderability. [1]–[4]. However, despite its advantages, the use of screen-printed Ag contacts has significant downsides. One of the most notable is its high cost, contributing up to 40% of the total cell production expense, posing a major barrier to scaling and achieving cost-effective solar cells [5]–[7]. Consequently, there is a pressing need to investigate alternative metals that have the potential to form ohmic contacts with Si substrate while reducing overall production costs. Metals such as copper (Cu) and nickel (Ni) have been extensively explored due to their similar conductivity and significantly lower cost compared to Ag [8]–[13]. Techniques such as plating, including electroplating and light induced plating, have emerged as promising methods for precise contact formation with these metals. However, the complexity of this process, including additional steps such as photoresist application, laser opening of Ni or Cu deposition, and the use of large amounts of consumables, adds to the fabrication cost and deviates from current manufacturing practices.

To maintain efficiency without increasing costs, it is crucial to adopt a metallization process that aligns with the state-of-the-art in its simplicity and high throughput. Printable metal pastes derived from Cu or Ni offer a potential solution, provided they can be adapted for fire-through applications. Prior studies have experimented with low-temperature curable Cu alloys or floating busbar designs [14]–[16]. However, these methods necessitate additional laser contact openings at the front surface and are often only applicable to certain grid designs such as floating busbars. In addition, the use of high temperature Cu pastes has been largely avoided due to Cu’s aggressive diffusion even at room temperature, except for recent studies of the Cu fire-through pastes, though these have yet to match the efficiency of their Ag counterparts [17]–[19]. Furthermore, directly contacting alternative metals such as Ni and Cu onto the Si emitter can potentially limit a solar cell’s power conversion efficiency due to recombination losses and contact resistance. To mitigate these issues, a seed layer capable of forming an ohmic-like contact with Si, is often placed beneath the metal bulk [10], [20], [21]. Ag is an ideal candidate for this seed layer, owing to its established role in the industry and the compatibility of its metal work function with the Si substrate.

Despite the extensive exploration of Cu and Ni as alternatives Ag in Si solar cells, this study introduces a novel approach by employing a screen printable fire-through technique for these metals, both with and without the inclusion of glass frit. This work further distinguishes itself by providing a detailed investigation into the composition of in-house metal pastes and their performance relative to commercial Ag paste. Additionally, we uniquely examine the influence of peak temperature on the fill factor for different contact designs, offering a comprehensive evaluation through an array of electrical assessments, thereby contributing a significant advancement to the field. Here in this study, we explore the fabrication of passivated emitter and rear contact (PERC) Si solar cells with stack contacts comprising of Ag seed layer topped with Ni and Cu bulk using screen printing. The use of three different in-house prepared fire-through pastes of Ag, Cu, and Ni is demonstrated here. These pastes are screen printed on the front surface of PERC cells to form the front contacts. Employing bi-layer contact structures of Ag/Ni and Ag/Cu not only presents a potentially effective alternative to Ag counterparts for highly efficient solar cells, but also results in significant cost reduction.

## Experimental Details

In the present study, passivated emitter and rear contact (PERC) solar cells were fabricated from silicon wafers possessing a resistivity of 2  $\Omega$ -cm. A silicon nitride (SiN<sub>x</sub>:H) layer with a thickness of 70 nm was deposited as an antireflection coating layer (ARC) layer on the front surface, and a 5 nm thick aluminum oxide (AlO<sub>x</sub>) layer along with a 75 nm thick SiN<sub>x</sub>:H layer were deposited on the rear side through plasma-enhanced chemical vapor deposition (PECVD). An aluminum (Al) contact was screen-printed on the back surface and subsequently dried at 200°C, followed by the application of front gridlines using three distinct metal pastes.

The first of these was a commercially available Ag paste, used as a reference for subsequent comparisons. The

second paste, an in-house Ag paste, was composed of Ag metal powder ( $\sim 3\mu\text{m}$  particle size), a glass frit, and an organic vehicle. The glass frit, prepared using the melt quenching method was constituted of 30-40% lead oxide (PbO), 25-35% tellurium oxide ( $\text{Te}_2\text{O}$ ), 22-26% bismuth oxide ( $\text{Bi}_2\text{O}_3$ ), 1-5% silicon dioxide ( $\text{SiO}_2$ ), 1-2% zinc oxide ( $\text{ZnO}$ ), 1-2% tungsten oxide ( $\text{WO}_3$ ) and 1-2% magnesium oxide ( $\text{MgO}$ ). The organic vehicle contained terpineol ( $\text{C}_{10}\text{H}_{18}\text{O}$ ) and texanol ( $\text{C}_{12}\text{H}_{24}\text{O}_3$ ) as solvents, ethyl cellulose and polyvinylpyrrolidone (PVP) as binders, hydrogenated castor oil as a thixotropic agent, and sorbitan-triolate as a surfactant. These components were blended in a weight ratio of 82.5:3.5:14 respectively, and the resulting mixture was subjected to three-roll milling for 60 minutes for proper dispersion.

The third paste employed was a Nickel (Ni) paste, prepared both with and without the aforementioned glass frit. The Ni paste, which included the glass frit, was prepared using the same glass frit and organic vehicle as the in-house Ag paste, but with a different weight ratio of components (77:3.5:19.5 for the Ni metal powder, glass frit, and organic vehicle, respectively). The Ni paste without the glass frit was prepared by combining Ni metal powder ( $4\mu\text{m}$  particle size) with the same organic vehicle in a weight ratio of 85:15.

Finally, a copper (Cu) paste was prepared without glass frit. It contained the same organic vehicle and was mixed in a weight ratio of 88:12 with Cu metal powder ( $2\mu\text{m}$  particle size).

Upon fabrication, the commercial Ag paste (Heraeus SOL9661) was applied to identical M2 wafers (with  $90\ \Omega/\text{sq}$  resistivity) to serve as a reference contacting mechanism. The printing was arranged according to the conventional H-pattern screen which has  $40\mu\text{m}$  openings. Other wafers of the same type were printed with the in-house Ag paste (single layer), Ni paste (single layer), as well as stacks of Ag paste + Ni paste and Ag paste + Cu paste. To measure the saturation current density and one of its components,  $J_{0\text{metal}}$ , according to [22], a special grid pattern containing different metal fractions is printed on a symmetrical sample divided into  $4\ \text{cm}^2$ -area cell size.

Following the preparation and printing of the different contact materials onto the wafers, a co-firing process was executed using a six-zone conveyor infrared (IR) belt furnace, adhering to the firing profiles outlined in Fig. 1. An exploration of various peak temperatures was conducted at a constant belt speed of 230 inches per minute (ipm) to understand the influence of peak temperature on the fill factor (FF) for different contact designs. Rapid rates of temperature increase and decrease were employed, as detailed in the inset graph of Fig. 1, in order to ensure uniform formation of the back surface field (BSF) on the rear side, and to enhance metal crystallite formation beneath the front contacts.

Upon completion of the firing process, the resulting solar cells underwent an array of electrical and optical assessments. Electrically, Suns- $V_{\text{OC}}$  measurements were performed to investigate resistive effects, ideality factor ( $n$ ), and saturation current density ( $J_0$ ). Light current-voltage (I-V) measurements were carried out to ascertain the maximum power, as well as the open circuit voltage ( $V_{\text{OC}}$ ) and fill factor (FF). Optically, the fabricated cells were examined via a scanning electron microscope (SEM) integrated with energy-dispersive X-ray (EDX) spectroscopy to visualize the cross section between the metal contacts and the emitter region of the solar cells.

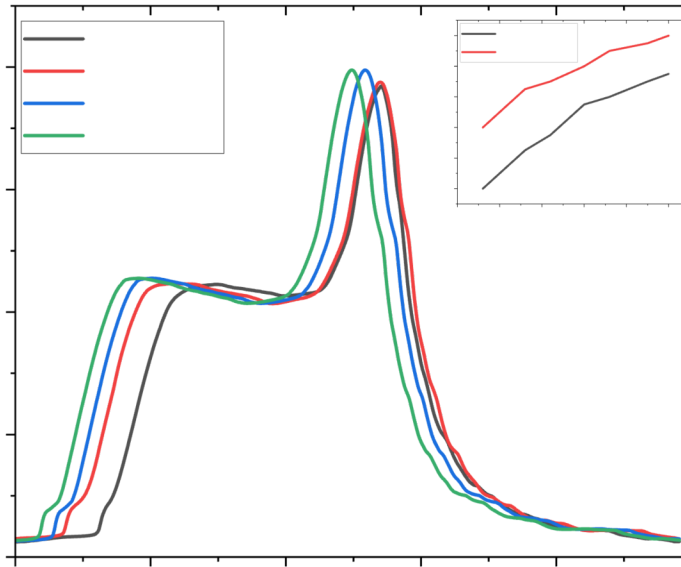


**Fig. 1** The contact co-firing temperature profiles with different peak temperatures. The inset graph shows the temperature velocity of the conveyor belt furnace for the profiles.

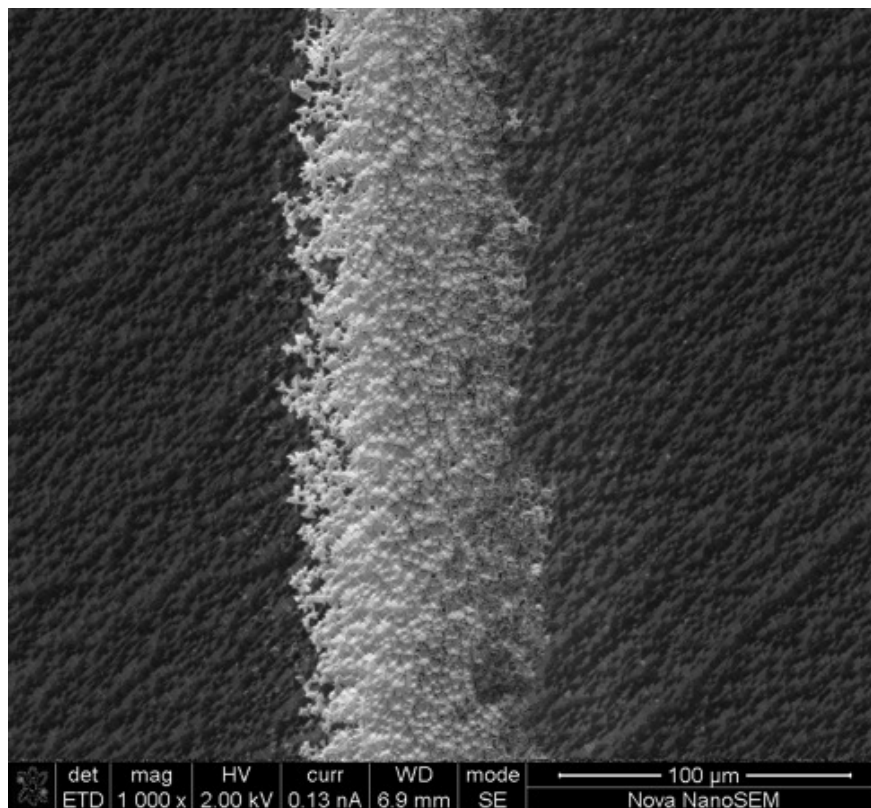
## Results and Discussions

Prior to the contact co-firing process, the average finger widths, as presented in Table I, fall within the range of  $51\mu\text{m}$  to  $55\mu\text{m}$ . Post-firing, the width of the Ag+Cu bi-layer stack notably expands to  $56\mu\text{m}$  due to most likely ductile behavior of copper, while concurrently attaining a height of  $10\mu\text{m}$ . Although the widths of the fingers shrink for each contact types, there is no ghost finger formation on the surface after firing process as shown in Fig. 2. In comparison, the width of the conventional screen-printed Ag contacts is slightly narrower. However, the metal fractions of the contacts, which are related to glass frit used in this study, are similar, measuring 5.1% for Ag, 5% for in-house Ag, 5.4% for the Ag+Ni bi-layer, and 5.7% for the Ag+Cu bi-layer, respectively. These are closely aligned with the approximated 5% metal fraction of commercial Ag contacts [23], [24]. As tabulated also in Table I, the width of the fingers varies depending on the metal used, a phenomenon potentially attributable to disparities in wetting and concentration within each paste. The Ni contact exhibits the narrowest average width of  $47\mu\text{m}$  post-firing, having commenced at  $55\mu\text{m}$  prior to the firing process. This highlights the increased tendency for Ni fingers to sinter and compact, forming into a continuous line. For the finger height of the printed fingers, contacts with in-house prepared Ag paste gives the tallest finger which suggests that the surfactant and thixotropic agent used in the paste, although the same type is used in each paste, correlate with Ag particles better than the others.

**Table I** The average finger widths and height before and after contact co-firing process

Contacts	Finger Width Before Firing ( $\mu\text{m}$ )	Finger Width After Firing ( $\mu\text{m}$ )	Finger Height After Firing( $\mu\text{m}$ )
Ag (reference)	53	49	9
Ag (in-house)	52	50	14
Ni	55	47	9
Ag + Ni	51	51	13

Contacts	Finger Width Before Firing ( $\mu\text{m}$ )	Finger Width After Firing ( $\mu\text{m}$ )	Finger Height After Firing( $\mu\text{m}$ )
Ag + Cu	55	56	10



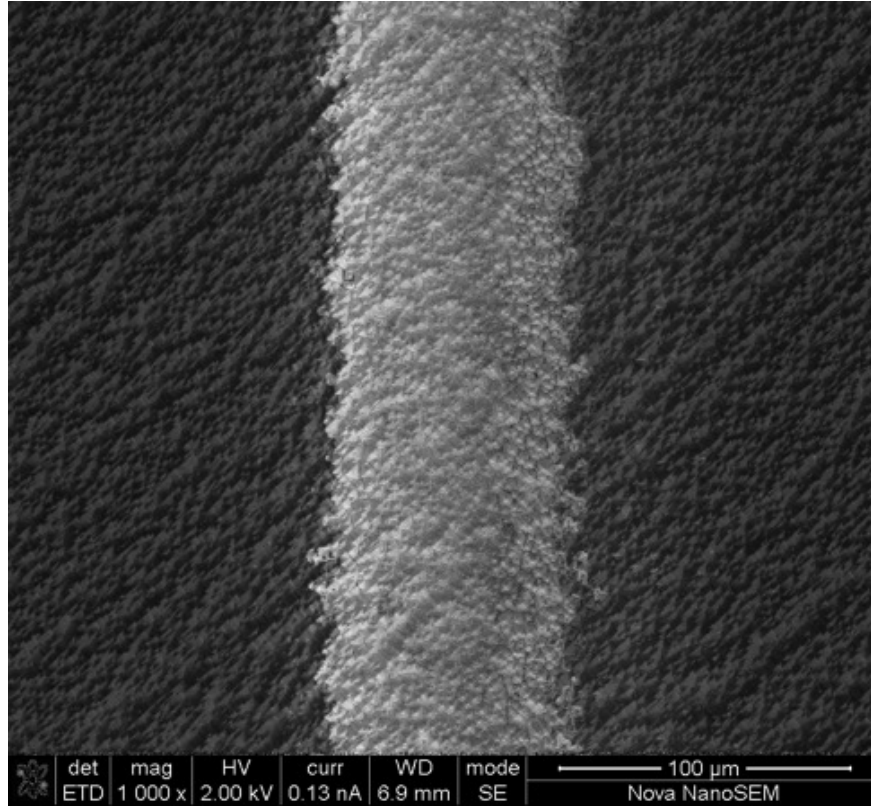


**Fig. 2** Top view SEM images of the two bi-layer stack contacts after firing

Supporting the above-mentioned premise, the results of finger resistance ( $R_F$ ) for the single layer Ni contact compared to the single layer Ag contact across different firing profiles, as depicted in Fig. 3a, demonstrate promising outcomes. Particularly, screen-printed Ni contacts at the industry-standard peak temperature of around 770-800°C (on the sample) exhibit favorable results in finger resistance compared to Ag counterparts. The  $R_F$  shows limited deviation with varying contact co-firing peak temperature, suggesting that metal particle sintering occurs properly for both Ni and Ag contacts. This can potentially be attributed to softening of Ni metals at the intersection of Ni/Si predominantly occur at elevated temperatures. Comparing the contact resistance of two single layer contacts, on the other hand, proves that Ag makes a better contact with Si than Ni as seen in Fig. 3b. This advantage stems from Ag's lower metal work function compared to Ni. The closer alignment of Ag's work function with Si's electron affinity ( $\sim 4.05$  eV) facilitates efficient charge carrier transfer across the metal-semiconductor interface, thereby reducing contact resistivity. Additionally, the relatively low contact resistance observed for both contact types suggests that the in-house prepared glass frit is effectively etching the ARC layer without damaging the emitter. This is further supported with power conversion efficiency and fill factor (FF) results of both single layer contacts, as shown in Figure 4. In line with the result of resistivity measurements of the contacts, the FF and the efficiency for Ni contacts suffer due to high series resistance thereby underscoring the potential of Ag as a viable seed layer.

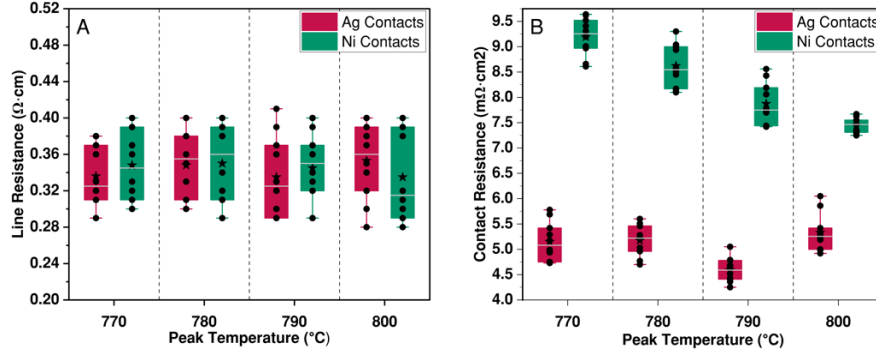


**Fig.3** The finger and contact resistances measurements according to different peak temperature of contact co firing for Ag and Ni contacts

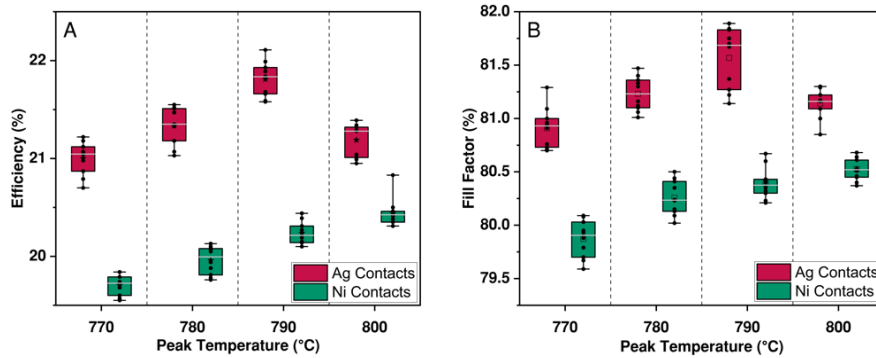


**Fig 4.** The efficiency and fill factor measurements according to different peak temperature of contact co firing for Ag and Ni contacts

To overcome the high contact resistivity of Ni and reduce the high cost of Ag contacts, Ag is used as a seed layer with Ni and Cu forming the bulk of the metal in a bi-layer contact type. The average electrical output parameters and the Suns- $V_{OC}$  measurement results for the single layer along with bi-layer contact types are presented in detail with respect to their optimized firing temperature in Table II. For reference, a screen-printed Ag contact solar cell is presented in Table III. The in-house prepared Ag paste performs the best among the other types with an average efficiency of 21.7%. The second best performing structure is Ag/Cu bi-layer contact stack which achieves 21.32% efficiency and FF of 81.4%. This result implies that even though the samples are fired at a peak temperature of 770°C, there is no Cu contamination in the cell, as supported by high shunt resistance ( $R_{SH}$ ) values of 150000. The  $J_{0, metal}$  value of 48fA/cm<sup>2</sup> and the  $R_C$  of 5.88mΩ[?]cm<sup>2</sup> for the Ag/Cu contact, compared to reference Ag contact of 41fA/cm<sup>2</sup> and 4.63Ω[?]cm<sup>2</sup>, also strongly indicate that Ag is successfully blocking the Cu diffusion into the junction. The total series resistance ( $R_S$ ) of the same contact, obtained by the light IV measurement, on the other hand, shows an additional resistive effect that may be due to the line resistance of the stack contact as a whole. This conclusion is further substantiated by the microstructure analysis depicted in Fig. 5. The elemental examination reveals that the Cu remains on top of the Ag layer, indicating that Cu, despite its aggressive diffusion properties, has not permeated underneath the Ag. The Ag/Ni contacts also result in promising electrical performance. The FF of 81.2% indicates that the contact formation is complete and there is no shunt in the cell considering the contact stack of Ag/Ni yielded close to maximum shunt resistance. However, the contact resistance and total series resistance is slightly higher than the others, possibly due to some delamination between Ag and Ni. For the Ni as a single contact, in addition to above-mentioned analysis, the cell is clearly shunted and degraded due to use of same glass frit in each paste and the peak firing temperature of 800°C, which is

clearly pushing the contact proximity closer to the junction. This is supported by the low shunt resistance of  $12050 \Omega[\?]\text{cm}^2$ .

**Table II.** The average electrical output parameters of best performed cells with respect to peak temperature

Metal Stack	$V_{OC}$ (mV)	FF (%)	$\eta$ (%)	$R_s$ ( $\Omega[\?]\text{cm}^2$ )	$R_c$ ( $\text{m}\Omega[\?]\text{cm}^2$ )	$J_{0, \text{metal}}$ ( $\text{fA}/\text{cm}^2$ )	$R_{SH}$ ( $\text{k}\Omega[\?]\text{cm}^2$ )	Peak ( $^\circ\text{C}$ )
Ag	665	81.7	21.72	0.54	4.63	51	150	790
Ag / Ni	661	81.2	21.14	0.76	6.41	53	131	780
Ag / Cu	663	81.4	21.32	0.65	5.88	48	150	770
Ni	654	80.1	20.44	0.84	7.42	98	12	800

**Table III.** The electrical output parameters of a screen printed Ag contacted reference cell

Type	$V_{OC}$ (mV)	FF (%)	$\eta$ (%)	$R_s$ ( $\Omega[\?]\text{cm}^2$ )	$R_c$ ( $\text{m}\Omega[\?]\text{cm}^2$ )	$J_{0, \text{metal}}$ ( $\text{fA}/\text{cm}^2$ )
Reference Ag Contacts	667	81.6	21.9	0.51	4.11	41

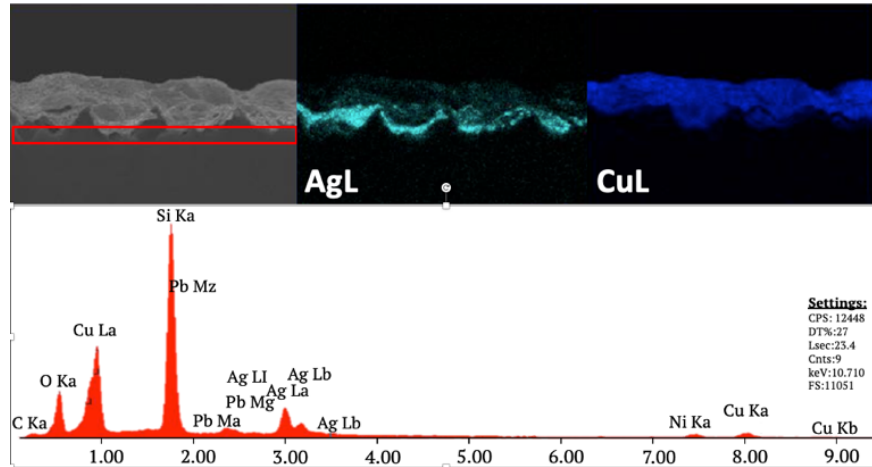
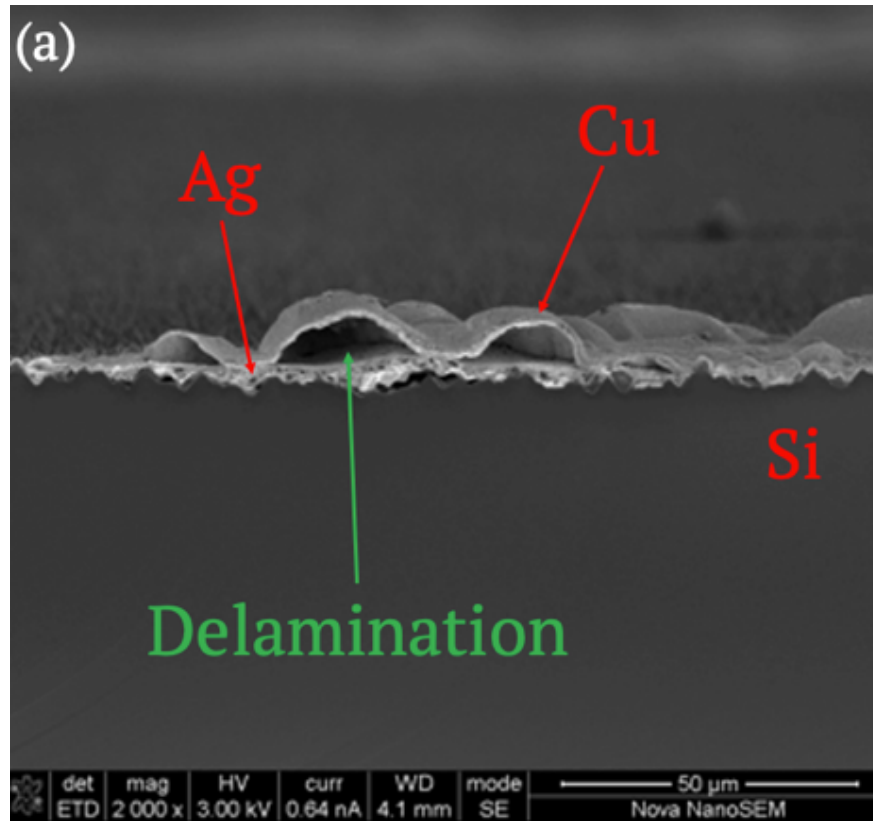
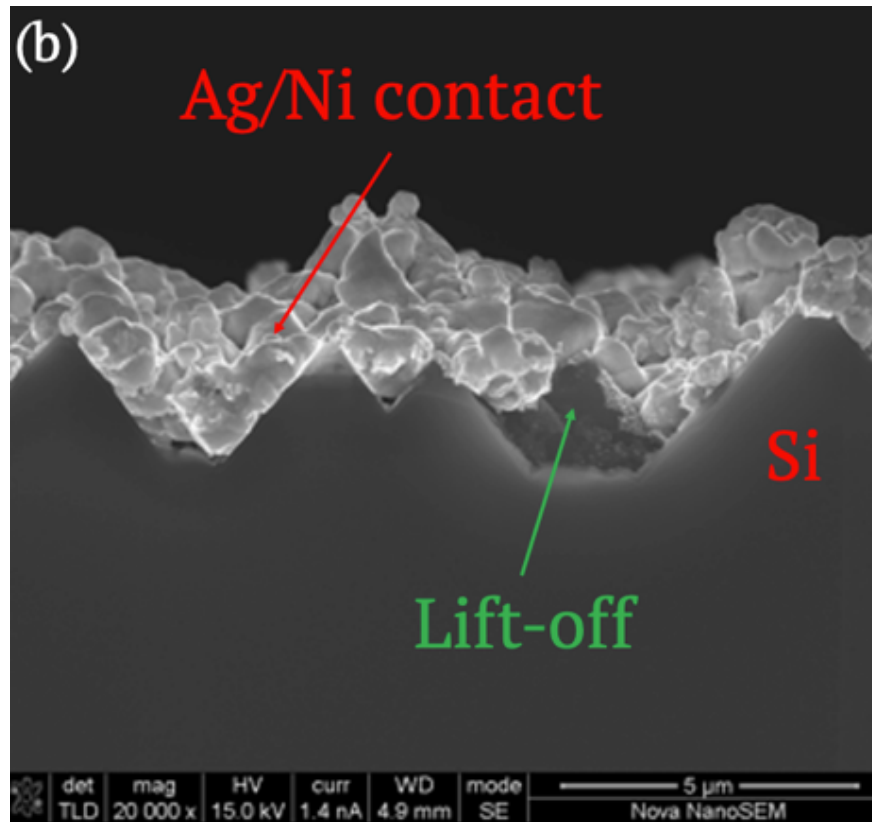


Fig. 5 Cross section elemental x-ray analysis of Ag/Cu contacts

Challenges in the printing process manifests themselves in two distinct forms; lift-off of Ag/Ni stack from the front surface and delamination of Ag/Cu contacts between the Ag and Cu. As illustrated by SEM images, these issues not only compromised the mechanical stability of the contacts but also influenced their electrical performance. Figure 6a provides a cross-sectional SEM image of an Ag/Cu contact after undergoing a contact co-firing process at  $780^\circ\text{C}$ . The clear separation between the Ag and Cu layers might be attributable to the differential thermal expansion of these metals during the firing process. However, this delamination issue is not apparent in contacts co-fired at peak temperatures below  $780^\circ\text{C}$ , underlining the significance of optimal firing conditions for the stability of these bilayer contacts. The SEM image in Fig. 6b exhibits a lift-off scenario with the Ag/Ni stack, where the contact stack detaches from the Si substrate in the middle, while remaining intact at the edges. This occurrence could stem from multiple factors, including differential thermal expansion, interfacial reactions, and inadequate surface preparation, among others. These observations align

with previous study [25], which reported similar lift-off and delamination issues in aerosol printed bi and tri stack layers of Ag frit/Ni and Ag frit/Ni/Cu when fired above 790°C peak firing temperature.





**Fig 6.** (a) SEM image of the Ag/Cu bi layer stack contacts after contact co-firing, the metals detached from each other created high line resistance and (b) SEM image of the Ag/Ni contact lifts off from the Si substrate

The efficiency and series resistance parameters, plotted based on finger width associated with lift-off and delamination in stacked contacts, are presented in Fig. 7. The results show that bi-layer contacts perform similarly to Ag counterparts, provide no delamination or a lift-off occur in the structure. Lift-off from the center damages the performance to the extent that the efficiency of Ag/Ni contacted cell may drop to as low as 16.62% as shown by the highlighted datapoints in Fig. 7 (left). The series resistance of those cells, shown in Fig 7 (right), may exceed  $1\Omega\cdot\text{cm}^2$  due to high contact resistance while delamination present itself as a finger resistance and increases the  $R_S$  for the Ag/Cu contacts. For those cells where the contact layers are intact, the contact resistance is in the range of the Ag reference, implying that the performance can reach industry standards and lower the Ag usage per watt. Following this data, it can be concluded that the performance of both Ag/Cu and Ag/Ni contacts closely mirrors that of their Ag counterparts. These findings suggest a high potential for these bi-layer configurations to serve as effective alternatives to Ag, especially considering their performance, which is commensurate with industry standards. By leveraging these alternatives, a considerable reduction in Ag consumption per watt can be achieved without compromising the efficiency of solar cells.

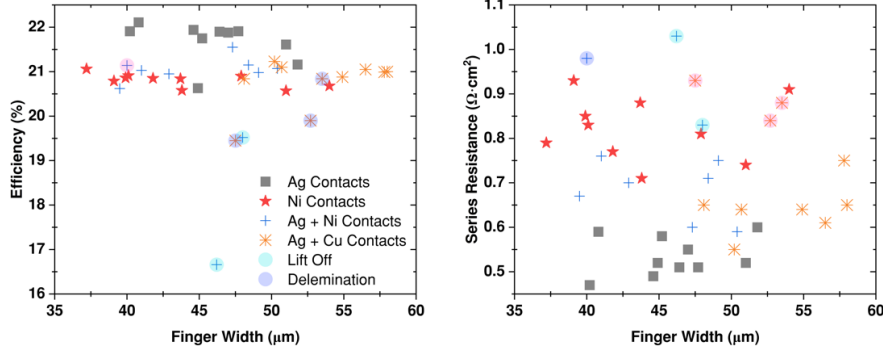


**Fig. 7** The efficiency and series resistance for different contacts with different finger width. Highlighting on the data point shows if the contact has a lift off or delamination, green highlight means lift off from substrate and pink means interlayer delamination.

One of the key determinants of the viability and scalability of the proposed alternative metallization technique is its cost-effectiveness and potential impact on the Levelized Cost of Electricity (LCOE). Prior research by Zhang [26] demonstrated that in traditional solar cell manufacturing, Ag consumption is around 13-20 milligrams per watt-peak (mg/Wp). This represents a significant cost due to the high market price of Ag, thereby posing a potential barrier to terawatt-scale production. In order to calculate the reduction in silver usage achieved through the employment of a bi-layer structure, using Ag as a seed layer and either Ni or Cu as bulk metal, all cells were weighed before printing and after co-firing the contacts, ensuring the complete removal of solvents and binders. The metallization patterns for each contact type were maintained consistent with 110 fingers and 5 busbars. The cells weighed for metal consumption analysis were carefully selected based on the average finger width, to minimize discrepancies between samples. The bi-layer contacts for consumption analysis underwent a two-step firing process: once after Ag printing, and once after Ni or Cu printing. This allowed for accurate determination of Ni and Cu consumption. As Table IV illustrates, the average values of Ag, Ni, and Cu consumption for the completed cells demonstrate that Ag consumption for bi-layer contacts is below 2.5mg/Wp. This represents nearly a sevenfold reduction when compared to the Ag contacted reference cell. Considering the Ag price of \$808, Ni price of \$24 and Cu price of \$8, the metallization cost per wafer drops 80.75% lower for Ag/Ni contacts and 82.15% for Ag/Cu contacts. The reflection of this cost drop on the LCOE is calculated according to Lazard’s calculation [27] with System Advisor Model (SAM) by NREL in a scenario in which it is assumed that M2 sized solar cells are used for 1GW solar farm in south Turkiye where the solar insolation is 5.1kWh/m<sup>2</sup>/day. The results show that for the reference Ag contacted solar cells yields an LCOE of 8.9¢/kWh. To analyze the effect of the bi-layer contacted cells on the LCOE, the sensitivity analysis is carried out in which the inputs are varied according to their electrical output parameters and metal consumption given in Table II and Table IV, respectively. Fig. 8 shows the sensitivity analysis results where negative correlation (to the left from the centerline) means lower LCOE and positive correlation (to the right from the centerline) results in higher LCOE. It is illustrated in Fig. 7 that although the loss in power conversion efficiency due to high series resistance has an impact to increase the LCOE around 0.35¢/kWh, the cost drop of metal consumptions has a higher impact to lower the LCOE of around 0.65¢/kWh. The increase in thermal budget for the contact firing of bi-layer contacts has a limited effect on the LCOE. Therefore, the financial implications of adopting this bi-layer metallization approach are significant. The drastically reduced silver consumption leads to substantial cost savings, which are directly reflected in the LCOE.

**Table IV** Ag Ni and Cu consumption of the finished cells after contact co-firing

	Ag reference cell	Ag/Ni contacted cell	Ag/Cu contacted cell
<b>Ag consumption</b>	91.5mg – 13.07mg/Wp	16.4mg – 2.41mg/Wp	15.9mg – 2.31mg/Wp

	Ag reference cell	Ag/Ni contacted cell	Ag/Cu contacted cell
Ni consumption		41.15mg – 6.04mg/Wp	
Cu consumption		-	44.9mg – 6.51mg/Wp

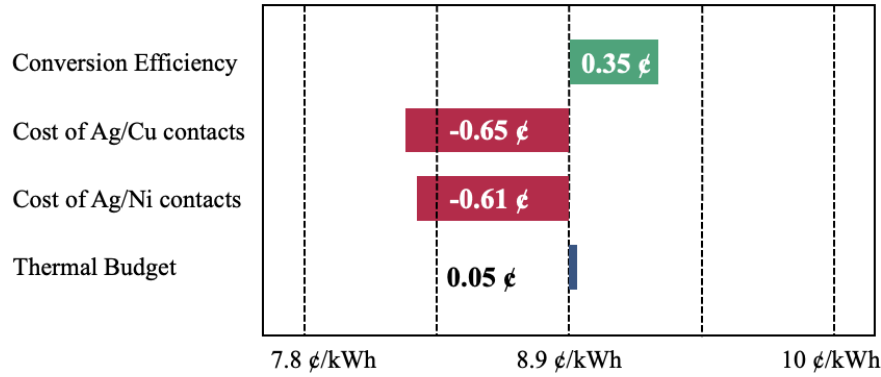


**Fig. 8** Sensitivity analysis of the LCOE for solar cells with bi-layer contact structure

### Conclusion

In conclusion, the adoption of the proposed alternative metallization technique, employing a screen printed bi-layer configuration with either Ag/Ni or Ag/Cu, presents significant advantages in terms of cost-effectiveness. These configurations, while maintaining a similar level of performance as traditional Ag contacts, substantially reduce the silver consumption and hence the overall metallization cost per wafer. Importantly, these cost savings are reflected in the Levelized Cost of Electricity (LCOE), showcasing the potential of this alternative technique to bring about notable cost efficiencies in the solar power industry. Although the efficiency loss due to higher series resistance and the slight increase in thermal budget for contact firing of bi-layer contacts are to be taken into account, the reduction in metal costs substantially outweighs these factors, resulting in a lower LCOE. This innovative approach, combining enhanced performance with economic viability, has the potential to significantly advance the manufacturing process of solar cells and bolster the broader transition towards more sustainable and cost-effective energy solutions.

### Acknowledgments

The authors would like to express their profound gratitude for the support provided by the Scientific and Technological Research Council of Türkiye (TÜBİTAK). This research has been made possible through grant, under reference number 120E474.

### REFERENCES

- [1] V. Unsur, N. Chen, and A. Ebong, “A mathematical investigation of the impact of gridline and busbar patterns on commercial silicon solar cell performance,” *Journal of Computational Electronics*, vol. 19, pp. 854–865, 2020.
- [2] A. D. Haigh, “Fired through Printed Contacts on Antireflection Coated Silicon Solar Cells,” 1976.
- [3] G. Schubert, F. Huster, and P. Fath, “Physical understanding of printed thick-film front contacts of crystalline Si solar cells—Review of existing models and recent developments,” *Solar energy materials and solar cells*, vol. 90, no. 18–19, pp. 3399–3406, 2006.
- [4] E. L. Ralph, “Recent advancements in low cost solar cell processing,” in *11th Photovoltaic Specialists Conference*, 1975, p. 315.

- [5] B. Hallam *et al.* , “The silver learning curve for photovoltaics and projected silver demand for net-zero emissions by 2050,” *Progress in Photovoltaics: Research and Applications* , vol. n/a, no. n/a, doi: 10.1002/pip.3661.
- [6] K. Branker, M. J. M. Pathak, and J. M. Pearce, “A review of solar photovoltaic leveled cost of electricity,” *Renewable and sustainable energy reviews* , vol. 15, no. 9, pp. 4470–4482, 2011.
- [7] P. J. Verlinden, “Future challenges for photovoltaic manufacturing at the terawatt level,” *Journal of Renewable and Sustainable Energy* , vol. 12, no. 5, p. 053505, Sep. 2020, doi: 10.1063/5.0020380.
- [8] G. Limodio *et al.* , “Copper-plating metallization with alternative seed layers for c-Si solar cells embedding carrier-selective passivating contacts,” *IEEE journal of photovoltaics* , vol. 10, no. 2, pp. 372–382, 2019.
- [9] A. Mette, P. L. Richter, M. Hörteis, and S. W. Glunz, “Metal aerosol jet printing for solar cell metallization,” *Progress in Photovoltaics: Research and Applications* , vol. 15, no. 7, pp. 621–627, 2007.
- [10] S. Glunz, A. Mette, M. Alemán, P. Richter, A. Filipovic, and G. Willeke, “New concepts for the front side metallization of silicon solar cells,” in *21st European photovoltaic solar energy conference and exhibition* , 2006, p. 8.
- [11] S. W. Glunz *et al.* , “Progress in advanced metallization technology at Fraunhofer ISE,” in *2008 33rd IEEE Photovoltaic Specialists Conference* , May 2008, pp. 1–4. doi: 10.1109/PVSC.2008.4922746.
- [12] A. U. Rehman and S. H. Lee, “Review of the potential of the Ni/Cu plating technique for crystalline silicon solar cells,” *Materials* , vol. 7, no. 2, pp. 1318–1341, 2014.
- [13] M. C. Raval and C. S. Solanki, “Review of Ni-Cu based front side metallization for c-Si solar cells,” *Journal of Solar Energy* , vol. 2013, p. 20, 2013.
- [14] M. Yoshida, H. Tokuhisa, U. Itoh, T. Kamata, I. Sumita, and S. Sekine, “Novel low-temperature-sintering type Cu-alloy pastes for silicon solar cells,” *Energy Procedia* , vol. 21, pp. 66–74, 2012.
- [15] D. Wood *et al.* , “Non-contacting busbars for advanced cell structures using low temperature copper paste,” *Energy Procedia* , vol. 67, pp. 101–107, 2015.
- [16] K. Nakamura, T. Takahashi, and Y. Ohshita, “Novel silver and copper pastes for n-type bi-facial PERT cell,” in *31st European Photovoltaic Solar Energy Conference and Exhibition* , 2015, pp. 536–539.
- [17] S. Huneycutt, A. Ebong, K. Ankireddy, R. Dharmadasa, and T. Druffel, “Understanding the Solar Cell Contacts With Atmospheric Screen-printed Copper,” in *2022 IEEE 49th Photovoltaics Specialists Conference (PVSC)* , IEEE, 2022, pp. 0937–0940.
- [18] N. Chen *et al.* , “Thermal Stable High-Efficiency Copper Screen Printed Back Contact Solar Cells,” *Solar RRL* , vol. 7, no. 2, p. 2200874, 2023, doi: 10.1002/solr.202200874.
- [19] D. Rudolph *et al.* , “Screen printable, non-fire-through copper paste applied as busbar metallization for back contact solar cells,” presented at the PROCEEDINGS OF THE 10TH WORKSHOP ON METALLIZATION AND INTERCONNECTION FOR CRYSTALLINE SILICON SOLAR CELLS, Genk, Belgium, 2022, p. 020006. doi: 10.1063/5.0127359.
- [20] M. C. Raval and C. S. Solanki, “Characterization of electroless nickel as a seed layer for silicon solar cell metallization,” *Bulletin of Materials Science* , vol. 38, pp. 197–201, 2015.
- [21] G. Limodio *et al.* , “Copper-Plating Metallization With Alternative Seed Layers for c-Si Solar Cells Embedding Carrier-Selective Passivating Contacts,” *IEEE Journal of Photovoltaics* , vol. 10, no. 2, pp. 372–382, Mar. 2020, doi: 10.1109/JPHOTOV.2019.2957671.
- [22] T. Fellmeth, A. Born, A. Kimmerle, F. Clement, D. Biro, and R. Preu, “Recombination at Metal-Emitter Interfaces of Front Contact Technologies for Highly Efficient Silicon Solar Cells,” *Energy Procedia* , vol. 8, pp. 115–121, Jan. 2011, doi: 10.1016/j.egypro.2011.06.111.

- [23] P. Padhamnath *et al.* , “Characterization of screen printed and fire-through contacts on LPCVD based passivating contacts in monoPoly<sup>TM</sup> solar cells,” *Solar Energy* , vol. 202, pp. 73–79, May 2020, doi: 10.1016/j.solener.2020.03.087.
- [24] M. Li, J. Wong, N. Chen, A. G. Aberle, and R. Stangl, “Determination of Metallization-Induced Recombination Losses of Screen-Printed Silicon Solar Cell Contacts and Their Dependence on the Doping Profile,” *IEEE Journal of Photovoltaics* , vol. 8, no. 6, pp. 1470–1477, Nov. 2018, doi: 10.1109/JPHOTOV.2018.2866177.
- [25] V. Unsur, T. Klein, M. F. van Hest, M. Al Jassim, and A. Ebong, “Rapid thermal processing of cost-effective contacts for silicon solar cells,” *Progress in Photovoltaics: Research and Applications* , vol. 27, no. 5, pp. 453–459, 2019.
- [26] Y. Zhang, M. Kim, L. Wang, P. Verlinden, and B. Hallam, “Design considerations for multi-terawatt scale manufacturing of existing and future photovoltaic technologies: challenges and opportunities related to silver, indium and bismuth consumption,” *Energy & Environmental Science* , vol. 14, no. 11, pp. 5587–5610, 2021, doi: 10.1039/D1EE01814K.
- [27] D. Ray, “Lazard’s Levelized Cost of Energy Analysis—Version 16.0,” p. 21, 2023.